Thermal Imaging of Breathing Patterns During CO Oxidation on a Pd/Glass Cloth

R. Digilov, O. Nekhamkina, and M. Sheintuch
Dept. of Chemical Engineering, Technion—Israel Institute of Technology, 32000, Haifa, Israel

Infrared (IR) thermography studies of oscillatory behavior during catalytic oxidation of CO over Pd supported on a glass-fiber catalytic cloth were conducted in a continuous reactor with feed flowing perpendicular to and through the disk-shaped catalyst. Typical thermograms of sustained patterns exhibit a hot spot that expands and contracts continuously (a breathing pattern), in a temporal pattern that matched the oscillations in exit CO_2 concentration. The oscillations were of the complex relaxation type, with fast (1-min) oscillations superimposed on the active phase of the long (10–60-min) cycle. The change in the number of these smaller peaks, with a varying parameter, corresponds to a period-adding scenario. A model based on a published kinetic (isothermal) oscillator for this reaction, coupled with a solid-phase enthalpy and gas-phase mass balances, predicts these main features of the pattern. The novelty of these experimental results lies in the pattern, which is well defined and amenable to a systematic mathematical modeling, in the short period of the fast oscillations, as well as in the catalyst geometry, a disk-shaped cloth. © 2004 American Institute of Chemical Engineers *AIChE J,* 50: 163–172, 2004

Keywords: IR thermography, heterogeneous catalysis, CO oxidation, glass fiber support, spatiotemporal patterns

Introduction

Problems of spatiotemporal patterns in catalytic reactors, caused by interaction of nonlinear kinetics with conduction, diffusion, or convection, have recently attracted considerable interest both theoretically and experimentally (see Sheintuch and Shvartsman, 1996, for a recent review in the field, and a recent *Catalysis Today* issue edited by Sheintuch and Jaeger (2002) dedicated to catalytic patterns). Multiple steady states and periodic or aperiodic behavior are quite common to catalytic and electrochemical reactions, as was demonstrated in numerous studies of these reactions (see reviews by Sheintuch and Schmitz, 1977; Schuth et al., 1993; Slinko and Jaeger, 1994). While the interaction of diffusion and a nonlinear reaction is known to induce a plethora of spatiotemporal patterns, the observations of well-defined patterns in heterogeneous reactors are still rare, and their identification in many cases is ambiguous due to experimental difficulties and nonuniformity of the system properties. The study of spatial structures in heterogeneous reactors is a challenging academic topic, yielding patterns that differ from those known to exist in reaction-diffusion systems exposed to uniform conditions, as well as a practical problem that should affect design and operation procedures of commercial reactors, like the catalytic converter or the fuel cell.

Catalytic and electrochemical reactors include several unique features:

- The interaction of the fluid phase, through which the reactants are supplied by convection, and the reactive solid phase, may produce patterns due to self-imposed gradients in the fluid phase. Patterns due to global (or nonlocal) interaction have been the subject of intensive research in the past few years (Sheintuch, 1989; Middya et al., 1993, 1994).
- Nonuniformity of properties, like catalyst loading and transport coefficients, are common to catalytic systems and may induce patterns (Sheintuch, 1996; Liaw et al., 1996; Annamalai, 1997).
- Boundary conditions that apply to many heterogeneous

Correspondence concerning this article should be addressed to M. Sheintuch at cermsll@tx.technion.ac.il.

reactors are different than the no-flux or fixed steady-state conditions commonly employed in studies of reaction-diffusion patterns. While this difference may not be significant for patterns with a large wave number, most reported patterns in catalytic systems typically show one or few fronts.

Aside from the catalytic wire, the foil or surface exposed to uniform gas-phase conditions is the simplest system to exhibit patterns. Understanding the patterns on these simple systems is crucial for predicting the behavior of a fixed-bed reactor. This article describes breathing oscillatory patterns, with temporally complex structures that were observed by IR thermography (IRT) in a simple catalytic system: a disk-shaped catalytic cloth, woven from glass-fiber and impregnated with Pd, through which a stream of CO, oxygen, and nitrogen was flowed. Our motivation in choosing this catalyst was its simple geometry and the low thermal capacity and low thermal conductivity that are associated with the 7–10 μm fiber. The surface density (g/cm^2) of this catalyst is two orders of magnitude smaller than that of a 4-mm sintered-glass disk, and this is also the reduction expected in the heat conductivity and heat capacity of the present cloth catalyst when compared with previously employed disk catalysts. The novelty of these results is in the cloth catalyst employed, the well-defined spatiotemporal pattern and in its relatively short time scale, and in the qualitative analysis and modeling of the behavior. The main features of the model, and its corroboration with results, are presented below. A detailed mathematical modeling of these results will be published elsewhere. A similar (but folded) Pd/cloth catalyst was employed in a mixed reactor by Yuranov et al. (2000), who reported on conversion isothermal oscillations only (that is, spatial patterns were not monitored); they mapped and modeled the domain of isothermal oscillatory behavior, and we use these results as a guide in searching for that domain. Our interest in cloth catalyst extends beyond the present application to abatement of water pollutants (for example, Matatov-Meytal and Sheintuch, 2002, which also presents micrographs of these catalysts) and to implementation as a diesel catalytic converter.

We review below some relevant experimental results. Patterns observed with catalytic wires or ribbons were well defined: moving and stationary fronts in uncontrolled systems may be sustained in a single variable reaction-diffusion (or conduction) model of wires or ribbons that catalyze a reaction with bistable kinetics. Stationary fronts are structurally unstable in one-variable systems, and their locus in the parameter plane separates domains with expanding upper state or by expanding lower state. Barelko et al. (1978), in a study of a Pt wire catalyzing ammonia oxidation, found an intermediate domain where structurally stable stationary fronts exist. Philippou et al. (1993) reproduced this experiment on a Pt ribbon using IRT, and showed that in the intermediate regime the front was not stationary, but moved at a very low velocity. The existence of stationary fronts, in a catalytic ribbon maintained at the preset average temperature, was verified by Lobban et al. (1989). Similar patterns were obtained under constant voltage control. Using IRT, Phillipou et al. (1991) observed temperature pulses moving back-and-forth, during propylene oxidation in a 14.5-cm-long Pt ribbon heated resistively under a constant resistance mode of operation. Cordonier and Schmidt (1989) presented a regular oscillatory pattern, in the form of two temperature pulses emanating in opposite directions from a source point, during ammonia oxidation on a Pt wire heated by a constant current.

Most patterns observed on two-dimensional (2-D) catalytic systems did not conform to any known motion of reaction-diffusion systems. Most investigators attribute the ambiguity to nonuniformity of surface properties. Several studies demonstrated the existence of one or more pacing centers that determine the motion of the whole surface. In several cases aperiodic solutions were shown to be associated with two or more such pacing centers. Considerable progress in elucidating and analyzing spatiotemporal temperature patterns was made with the employment of IRT: Kellow and Wolf (1991) observed that active hot zones on a Rh/SiO_2 surface catalyzing ethylene oxidation were contracting and expanding. Spatiotemporal dynamics on supported catalysts can be presented as the interaction of "coherent" structures induced by long-range nonuniformity. For the same system Chen et al. (1991) employed orthogonal decomposition of IRT snapshots to describe hot-spot flickering, which caused ignition of the second active spot, and hot-spot wandering over the support. Graham et al. (1993) used IRT to monitor thermokinetic oscillations during hydrogen oxidation on 3.8-cm nickel disk. They showed two pacemakers at the edge of the disk, emitting ignition-fronts, which conquers the surface within 40 s. After a slow cooling, which was not associated with front motion, new fronts originated at the pacemakers' positions.

Well-defined rotating patterns were observed on catalytic rings and cylinders: continuously moving pulses were observed during hydrogen oxidation on a nickel ring suspended in a stirred-tank reactor, kept in a constant-temperature oven (Lane et al., 1993). Rotating patterns were observed during CO oxidation on a cylindrical Pd catalyst (Marwaha et al., 2001).

Oscillations in high-pressure reactions are due to autocatalytic thermal effects, autoinhibition by a reactant, and the slow reversible changes of nondiffusing catalytic activity. In such a model, the thermal-conduction range is larger than the diffusion scale of any surface species. The expected behavior is thus similar to that in an excitable medium in which, if a traveling pulse is formed, it propagates out of the system; in the absence of control or global interaction, the system eventually attains a uniform state. This mechanism is contrary to most mathematical models of pattern formation that, following Turing's classic analysis, incorporate a localized autocatalytic variable (activator) and a far-reaching inhibitor. The patterns just reported for high-pressure catalytic reactions are different from the target patterns and spiral waves that were encountered in liquid-phase reacting systems, in physiological systems like the heart muscle and eye retina, and on a single isothermal platinum crystal catalyzing the low-pressure oxidation of carbon monoxide (Ertl, 1990).

Experimental Setup and Procedure

Experimental system

The reaction was conducted in a specially designed cylindrical aluminum reactor of 42-mm inner-diameter and 70-mm depth with wall thickness of 5 mm (Figure 1). The aluminum catalytic reactor (see Figure 2) was housed in a thermally insulated electrical oven (model CARBOLITE, PF30) with a 9-L volume with controlled temperature. The reactor has a

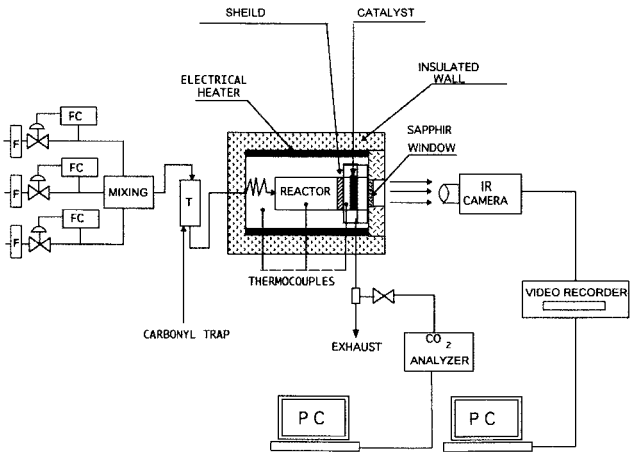

Figure 1. Experimental system.

sapphire (ISP Corporation) window of 38 mm in diameter for IR viewing.

The feed gases used were prepurified CO (99.9%, Linde), extra-dry oxygen (99.6%, Linde), and high-purity nitrogen (99.999%, Linde), supplied from cylinders into three pipelines and further purified on-line (Molecular Sieve 4A, Linde) to remove any moisture traces in the feed. Three sets of mass flow controllers (Brooks 5850S with Control & Read Out Unit Brooks Microprocessor 0152/0154) operated on each line and generated the desired composition and kept the flow rate constant with an accuracy of better than 1%. The three lines ended in an aluminum cylinder where the feed gases were mixed, and the mixture was passed through a hydrocarbon trap (Molecular Sieve Adsorbent, Linde) to remove any hydrocarbons. The mixture was preheated in the oven by passing it through a spiral tube leading to the reactor through the bottom inlet port (Figure 2). The product gases exited through three angular symmetric outlet ports on the top flange (see Figure 1).

The catalyst, GFC impregnated with Pd, in the form of a woven circular disk was fixed by 38-mm aluminum rings between the inlet and outlet ports parallel to an infrared-transparent sapphire window. The infrared-transparent lid allows the catalyst to be viewed during the reaction from the direction opposite the feed port. The temperature in the reactor was measured by thermocouple and kept constant (within 0.5°C) by a PID controller (TFC-400). The reactor operated at atmospheric pressure. The vessel temperature was measured by a second thermocouple. A third thermocouple was placed under the catalyst near its center.

The CO oxidation was studied mainly over a 0.6 wt. % Pd/GFC in a temperature range of 210–254°C, with CO varying in the feed from 0.1 to 2 vol %. The oxygen inlet concentration was kept at 20 vol %. An infrared gas analyzer PGA/EDG/NA measured the composition of vessel effluent CO_2 concentration.

Imaging and data analysis

The IRT of the catalyst surface during the reaction was monitored with a high-resolution infrared video camera (THERMACAM PM350) positioned about 25 cm from the catalyst surface. The camera has a 256 × 256-pixel platinum silicide focal array (FRA) detector, which provides a superior image with a spatial resolution of 0.5 mm and a scale resolution of 0.1°C, without the use of mechanical scanning. An integrated closed-cycle cryogenic cooler maintains the detector temperature. Images were displayed on a color LCD viewfinder, and can be output as Standard-Video or S-Video. Image analysis was performed with static images transferred to AGEMA software via the PCMCIA ImageBank memory card. The IR camera has an internal compensation and self-calibration system based on two micro-blackbodies and four temperature sensors. It is thermoelectrically cooled and operates in the shortwave range of 3–5 μm, which makes it suitable up to 450°C applications. The camera was equipped with two zooms to vary the spatial resolution of the images.

The IR camera was connected to a video recorder and interfaced with a PC for the on-line acquisition; AGLEAM-Researcher-2000 software was used for thermal mapping in the catalyst-array, 12-bit digital image data. The emissivity value of the GFC surface, determined by adjusting to a thermocouple reading in the absence of the reaction, was $\epsilon \approx 0.7$.

For the purpose of monitoring and control, IR images were displayed at 25 frames/s on a PC and video monitor in real time, and the NTSC signal was also recorded by a videocassette recorder ("Umatic" SONY VO-5800PS). The images were transferred from video to digital format (tiff) and stored on the hard disk of the Pentium-3 PC for later analyses. In the image analysis and digital data storage mode the catalyst area was scanned every 2.5 s.

Preparation and characterization of catalyst

Commercial aluminaborosilicate GF in the form of woven fabrics, known as E-type and produced by "Steklovolokno," Polotsk, Belarus, were used as a catalytic support. A typical composition of EGF consists of 54% silica (SiO_2), 16.5% calcia (CaO), 14.5% alumina (Al_2O_3), 10% boron oxide (B_2O_3), and 4% magnesia (MgO). The material was made from long threads of elementary bundled filaments (diameter 7–15 μm). The specific surface area of EFG fabrics was about 1–2 m^2/g. Details of the preparation of noble metals supported catalyst on woven GF fabrics were reported elsewhere (Shindler et al., 2001).

To remove impurities contained in commercial GFC the cloth was washed by water and dried in air at 80°C. In order to create surface roughness and develop porosity the starting material was treated with aqueous solutions of HCl. The strong acid attacks the surface, leaching out the nonsilica components. The sample was then rinsed in distilled water and dried on air at 80°C.

Palladium(II) chloride ($PdCl_2$, purum, Fluka) was used as a

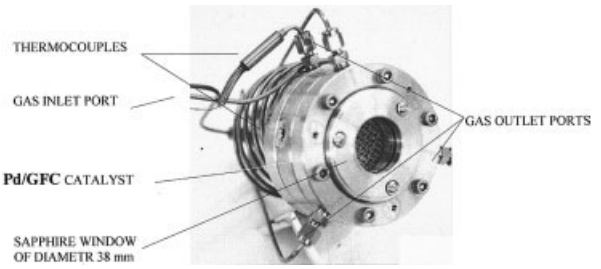

Figure 2. The reactor and its components.

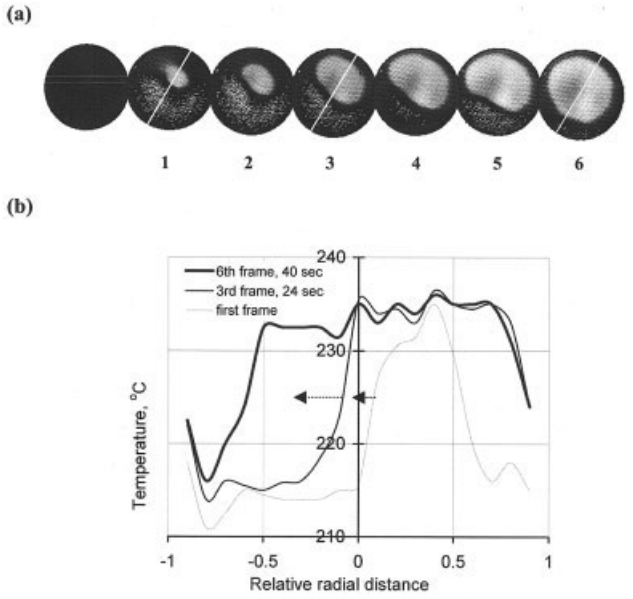

Figure 3. Typical oscillatory breathing pattern showing a sequence of snapshots over 40 s (upper row), temperature distribution in the indicated cross section (lower row; for the corresponding CO_2 effluent concentrations see Fig. 4a).

Conditions: Feed flow rate of 1 L/min; 1.4% CO in feed; reactor temperature is 214°C; 0.35% Pd/GFC catalyst.

precursor for the metallic palladium catalyst. The Pd-supported catalyst was prepared by the Pd deposition on a GFC via impregnation from an aqueous solution of hexachloropalladium acid (pH 2.2) or $PdCl_2$ with ammonium hydroxide (pH 10), with appropriate concentrations to obtain palladium loading in the range of 0.05–1.0 wt. %. The samples were then dried overnight at 70°C, washed, and calcined at 450°C air for 1 h. After reduction in H_2 at 200°C for an hour, the catalyst was ready to be used.

The catalyst Pd-content was determined in wt. % spectrophotometrically by Inductively Coupled Plasma Emission Spectrometry (Perkin-Elmer Optima 3000 DV instrument) after dissolving Pd/GFC samples in concentrated HNO_3 and analyzing it. The total content of Pd was varied from 0.4 wt. % to 1.0 wt. %.

Results

We describe below the basic features of the pattern, by portraying the time-dependent IR image and the corresponding conversion, and then we present a bifurcation diagram with varying oven temperature. Parameters that varied in the experiments were the reactor temperature, feed concentration, and flow rate. Here we present only the effect of the reactor temperature. While we have studied the dynamic behavior over a variety of catalysts, which differ in their Pd loading and GFC features, the results presented here, which employed only two catalysts (one in Figure 3 with 0.35% Pd/GFC and another with 0.6% in all others), were typical of most others.

Figure 3 shows a sequence of typical thermograms of patterns in the active fraction of the cycle, plus several cross sections. The basic feature of these patterns is a breathing motion by a hot spot that expands and contracts continuously in a cycle that lasts 1–2 min. This behavior is accompanied by complex relaxation oscillations of the CO_2 concentration, with an overall period of about 10–60 min, and composed of an active and an inactive section; the active section is superimposed with several small-amplitude high-frequency peaks with a period of 1–2 min (Figure 4a, bottom) that correspond to the sequence shown earlier. Along the inactive section (crest), the catalyst is completely cold and uniform, while in the active state the hot spot expands and contracts. While the surface is not completely uniform, the hot spot expands in all directions over the catalyst surface. The displayed figures characterize one small cycle out of several peaks that are evident in the temporal changes in conversion. A gray-scale spatiotemporal pattern (that displays the square-root of the fraction of the

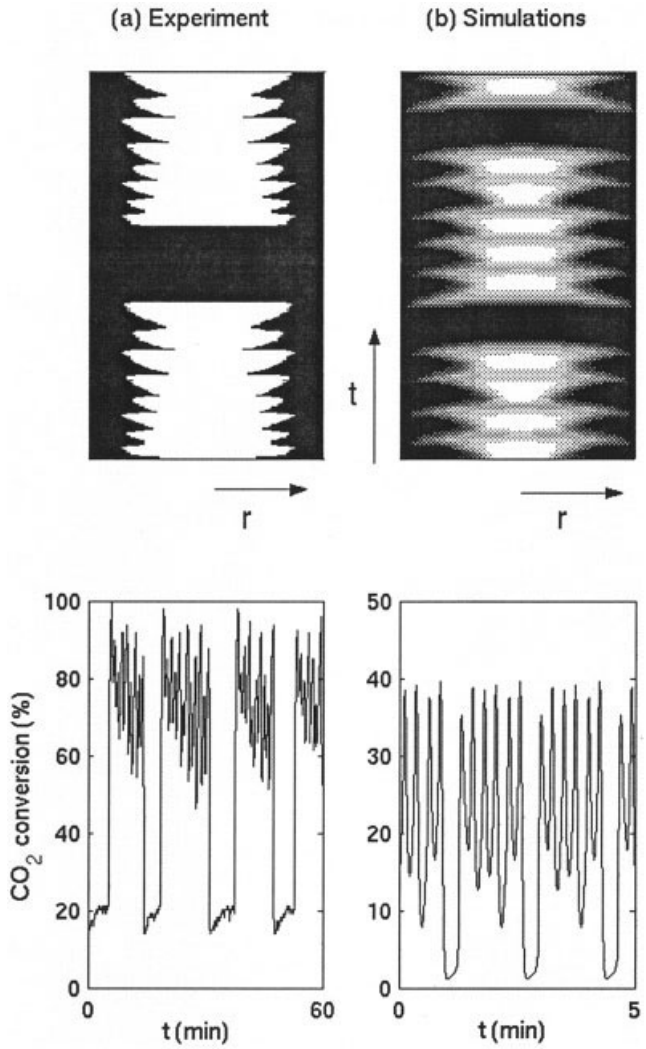

Figure 4. (a) Experiments vs. (b) simulations: upper row presents gray-scale spatiotemporal presentation of the (square root of the) active fraction of the surface.

Lower row presents CO_2 effluent concentrations indicating the three time scales of the problem, of the data presented in Figure 3. Simulations were conducted using the model outlined in the text with $P_{CO} = 750$ Pa (0.75%) and $T_g = 220$°C ($\Delta T_m = 150$°C, $B = 0.005$; other parameters, see text).

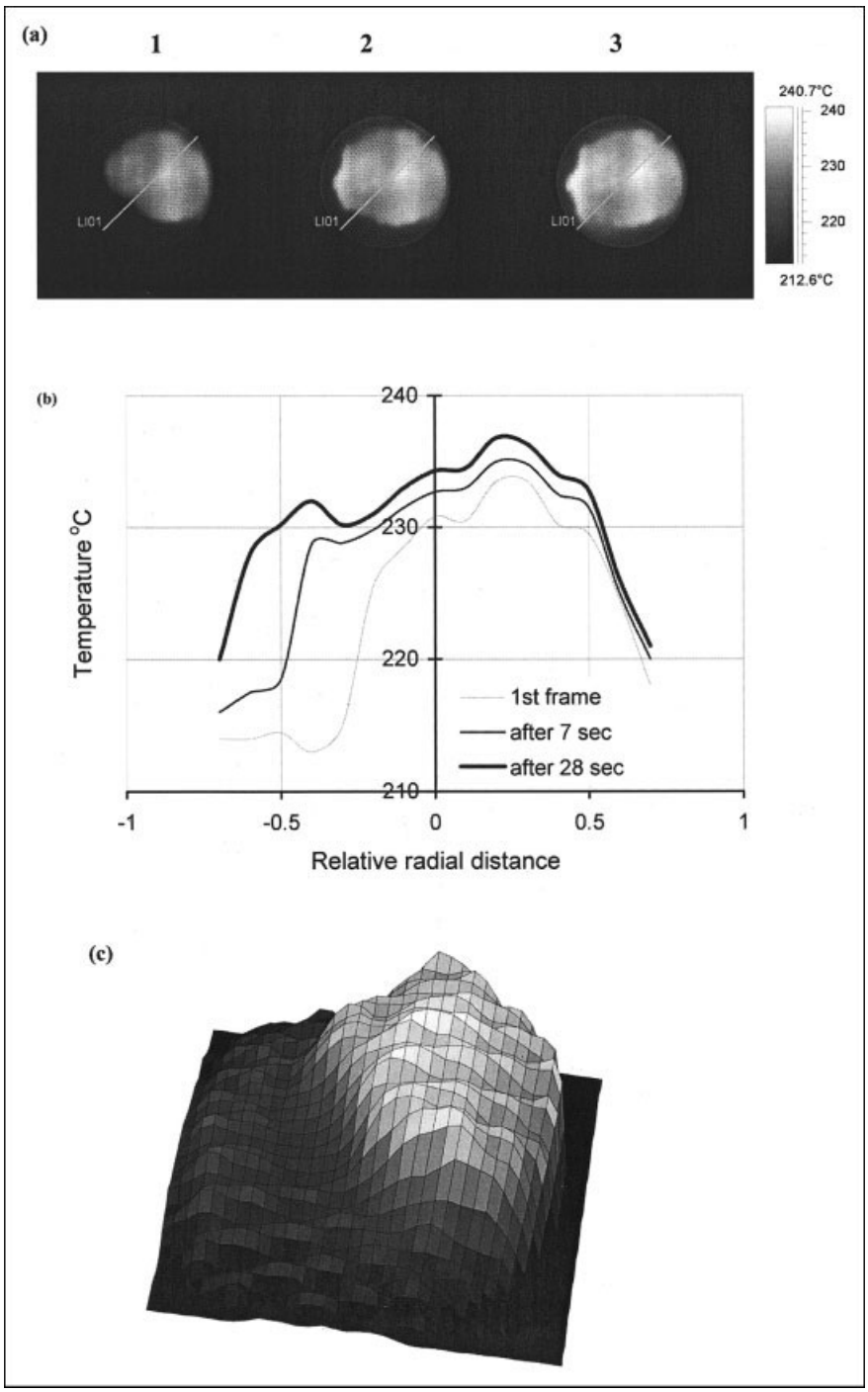

Figure 5. Another typical oscillatory breathing pattern showing (a) sequence of snapshots over 28 s, (b) temperature distribution in the indicated cross section, and (c) a 3-D representation of one snapshot.

Conditions: Feed flow rate of 1 L/min; 1.0% CO in feed; reactor temperature of 218°C and 0.65% Pd/GFC catalyst.

surface that is in the active-state) is presented in Figure 4a, top. (It is presented around the center and it does not show the asymmetric nature of the pattern; that will require animative presentation.) There appears to be a correlation between the area of the hot domain and the conversion.

One-dimensional cross sections of the surface temperature (Figure 3b) exhibit spatially active and inactive domains of the 36-mm disk, separated by a relatively steep front. The temperature difference between the two domains is about 20°C. The front velocity is 1 cm/min in order of magnitude. The hot spot is not central to the disk, and consequently the front velocity varies with position.

Another sequence of states, with corresponding one-dimensional cross sections, is shown in Figure 5 along with a 3-D presentation of the temperature. Again, the temperature difference between the cold and hot domain is relatively small (about

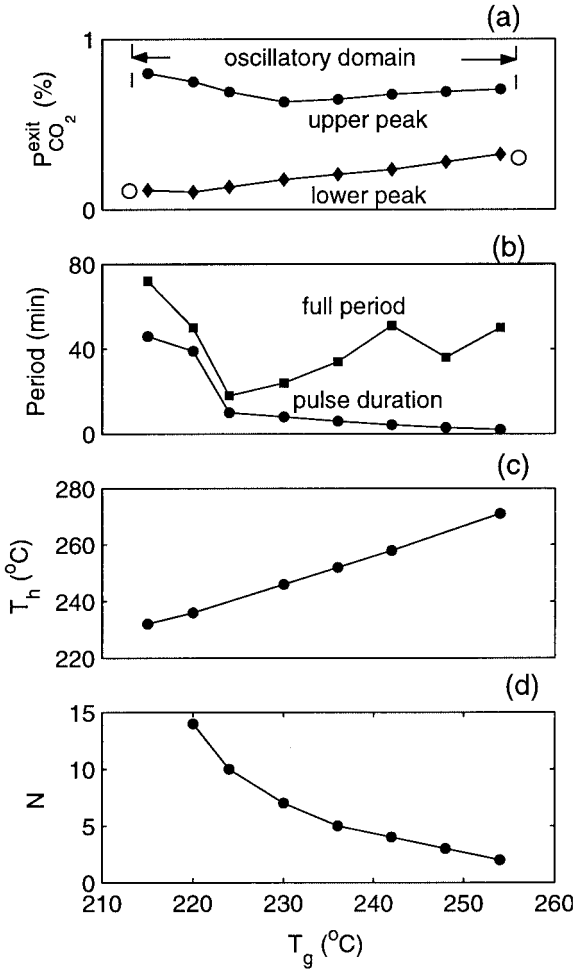

Figure 6. Bifurcation diagrams with varying reactor temperature showing (a) the amplitude of effluent oscillations, (b) the duration of the period and of the active phase, (c) the temperature at the hottest spot (T_h), and (d) the number of high-frequency cycles in the active phase of the cycle (N) (conditions as in Figure 5a).

15–25°C), but the boundary is relatively sharp in the form of a front. The temperature of the hot domain is not uniform.

Bifurcation diagram with varying reactor temperature

After attaining a fully ignited state, the vessel temperature was decreased or increased stepwise until the oscillations disappeared. At each reactor temperature we waited 1.5–2.0 h before recording IR images. For a feed flow rate of 1 L/min and a CO feed concentration of 1 vol. % the spatiotemporal patterns were observed in the 215–254°C temperature range. At temperatures, below 215°C and above 254°C the reaction rate was very small, and a stable uniform extinguished state existed. The degree of the conversion of CO was below 100% in this experiment, and the conversion matched the behavior of thermal patterns.

The bifurcation diagram with respect to reactor temperature (Figure 6) shows the domain of oscillatory patterns, the endpoints of the conversion amplitude (a), the approximate period of the oscillations and duration of the active section of the cycle (the pulse, b), the hot-spot temperature (c), and the number of small-amplitude peaks in the active zone (d). The oscillations seem to disappear by a hard (discontinuous) bifurcation upon increasing or decreasing temperature; this observation is supported by the observation of increasing periods at high temperatures. The change in the duration of the active zone, from conditions where it captures more than half a period at low temperatures to conditions where it lasts only 1/20 of a period, is typical of models of relaxation oscillations. While the number of small peaks varied somewhat from one period to the other, this variation was at most by one (e.g., 3 or 4 peaks per cycle). The consistent trend in the number of small peaks (Figure 6d) is surprising, suggesting that another frequency is important.

Also shown in the figure is the temperature of the hot domain (Figure 6c), showing that the difference between the hot and cold domains is almost constant, independent of the oven temperature. This suggests that at the hot domain the reaction rate, per unit catalyst area, is constant and is limited by kinetics or by mass transfer.

In the absence of a complete presentation, we show a sequence of thermograms (Figure 7) that correspond to the upper and lower CO_2 peaks at several reactor temperatures. Recall again the relaxation–oscillation nature of the conversion oscillations (two charts are plotted in Figure 8), which are superimposed with fast oscillations over the active phase. Several plots of the active section of the cycle are plotted in Figure 9, showing again that the active section is long at low temperature, accompanied with a large number of fluctuations, while the situation is reversed at high temperatures. Comparison of the thermograms (Figure 7) and the active phase of the CO_2 profile (Figure 9) shows that the disk is neither fully ignited at the upper peak nor fully extinguished at the lower peaks of the small-amplitude oscillations. It becomes extinguished in the inactive section. The thermograms suggest some nonuniformity that repeats itself at all temperatures. To make the discussion concrete, compare the thermograms recorded in Figure 7 at 254°C with the corresponding peaks at Figure 9: the second thermogram (at 0.29 min) shows a nonuniform distribution with a hot spot at 270°C, surrounded by a relatively warm perimeter; the corresponding conversion is 95% (Figure 9). The next thermogram (1.32 min), recorded at a lower conversion peak (60%), shows a contracted hot spot and a cooler perimeter. The next upper peak (3.16 min) shows a somewhat lower conversion and a somewhat smaller hot spot (compared with the state at 0.29 min). As the temperature is decreased to 242°C, there are four upper peaks (and three lower ones, aside from the inactive section) that look qualitatively similar but are quantitatively different.

Discussion and Modeling

The following are the main features of the observed patterns and oscillations: the main feature is the breathing pattern that was observed in all oscillatory states. Such a pattern usually implies the existence of a stationary front solution, which is unstable in its position and oscillates around it. The second feature is the nature of the conversion patterns that are of the relaxation–oscillations type; the thermograms in Figure 9 show only the section of the period with high activity. A third feature

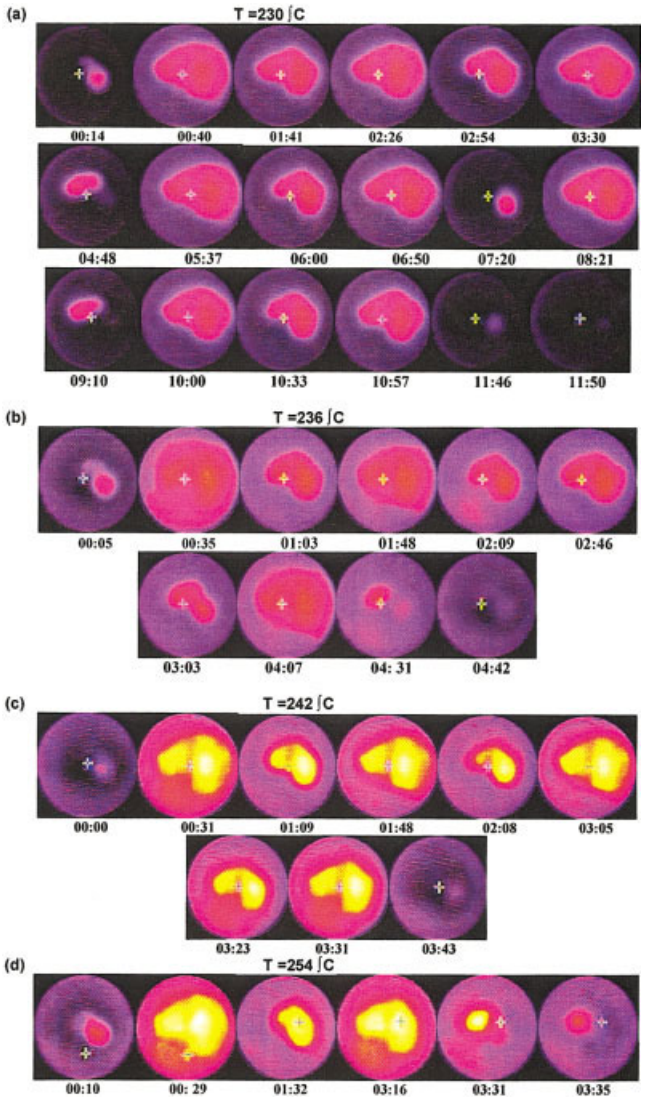

Figure 7. Patterns corresponding to the upper and lower effluents CO_2 peaks at four temperatures (conditions as in Figure 5a; temperature is denoted).

of these patterns is that the conversion (that is, CO_2) oscillations are complex, multipeak (also termed mixed-mode, for example, Sheintuch and Luss, 1989), and are usually aperiodic in the sense that the details are not reproduced exactly from one period to another. The fourth feature of the observed oscillations is that three time scales are evident in the system: the turnover frequency is less than 1 s in order of magnitude, the period of the relaxation oscillations ranges from 10 to 60 min, while the fast superimposed oscillations have a period of about 1 min. A fifth feature we identified is the period-adding mechanism that accounts for the change in the number of smaller peaks in a cycle (Figure 6); this mechanism was identified in a variety of reaction engineering problems (Elnashie et al., 2001). A more careful inspection when plotting the number of small peaks vs. a parameter should reveal a staircase diagram interrupted by chaotic windows (Coombes and Osbaldestin, 2000). Another feature of the observed oscillations is the nonuniformity of the pattern, which is probably due to the

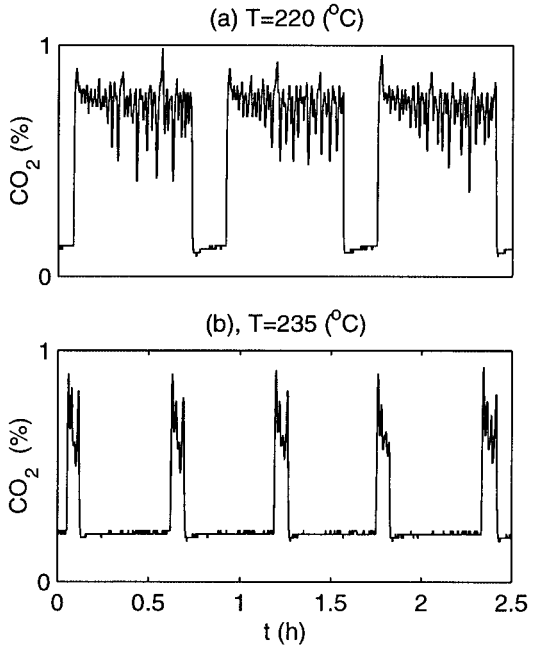

Figure 8. Two typical oscillatory profiles of effluent CO_2 (conditions as in Figure 4a; temperature is denoted).

nonuniformity of catalytic activity and of catalyst loading. The last feature we note is that the temperature gradient between the hot and cold domains is constant for the data shown in Figure 6. In other experiments, it ranged from relatively few degrees at low gas feed and low CO concentration (0.5 vol. %) up to

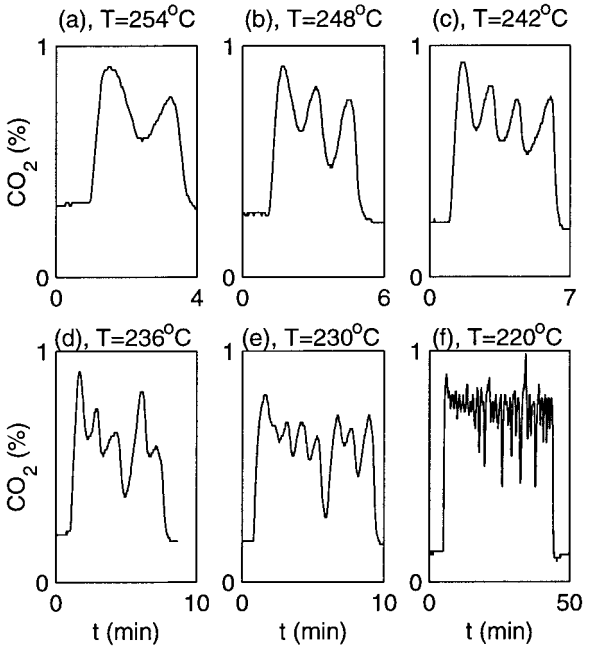

Figure 9. Oscillatory profiles of effluent CO_2 during the active phase of the cycle, at various temperatures (conditions as in Figure 5a; temperature is denoted).

some tens of degrees at high gas feed (1–2 L/min) and high CO concentration (1–2 vol. %).

We now discuss the structure of the mathematical model that may account for these observations. We argue that the model should have the following features: (1) it should incorporate a fast activator and a slow inhibitor; (2) the inhibitor in catalytic systems is typically a surface concentration and does not diffuse, which rules out the most common (Turing) mechanism for pattern formation; (3) the distributed model should be subject to boundary conditions of fixed temperature or mixed conditions at its perimeter; and (4) a certain nonuniformity of activity or conditions should be incorporated. Activator–inhibitor models are frequently employed in modeling catalytic oscillations and account for relaxation oscillations (see reviews cited in the Introduction). The activator is the CO or oxygen surface coverage in isothermal models, while in nonisothermal conditions the temperature plays an important role; it is reasonable to assume that, due to the low temperature differences between the hot and cold zones observed here, the oscillations are driven by kinetic effects, which are reflected by temperature oscillations (e.g., Keren and Sheintuch, 2000). Thermal effects are important, however, since information is conveyed by conduction, and heat capacity stabilizes the motion. The inhibitor nature is still debated, but most models assume it is the degree of Pd oxidation. As explained in the Introduction, such an activator–inhibitor system with a localized inhibitor will typically yield homogeneous steady and oscillatory states in systems with uniform properties, and will not account for a stationary or oscillatory front. Rotating patterns may emerge with special asymmetric initial conditions (Sheintuch and Nekhamkina, 1997). Patterns may emerge due to global coupling, which may be induced by the interaction through the fluid phase, but the observation that patterns persist even at small conversions suggests that this effect is not overwhelming.

In another article (Nekhamkina et al., 2003), we outline the main considerations in constructing a mathematical model for the data. We review various mechanisms in the literature that were employed for constructing breathing patterns, to show that they do not apply here. The thermograms strongly suggest that the boundary temperature is always low, and due to the inert nature and large heat capacity of the ring that holds the cloth, we need to impose fixed-temperature boundary conditions, forcing the edge to be at the reactor temperature, or mixed conditions with a high heat-transfer coefficient at the edge. In that article we show that this boundary condition repels the front and will lead to symmetric breathing patterns. To account for the asymmetry we need to assume the nonuniformity of a certain parameter, like activity.

The mathematical model studied in Nekhamkina (2003) is based on a published oscillatory kinetics model [the STM model (Sales et al., 1982), which was modified later by Slinko et al. (1999)] and is coupled there with an enthalpy and gas-phase balances. The surface kinetic model is described by

$$\frac{dx}{dt} = k_1 P_{\mathrm{CO}}(1 - x - y) - k_{-1}x - k_r xy - [k_4 xz] \qquad (1a)$$

$$\frac{dy}{dt} = k_2 P_{\mathrm{O}_2} e^{-\alpha z}(1 - x - y)^2 - k_r xy - [k_3 y(1 - z)] \qquad (1b)$$

$$\frac{dz}{dt} = k_3 y(1 - z) - k_4 xy \qquad (1c)$$

where x and y are the concentration of adsorbed carbon monoxide and adsorbed oxygen, respectively, and z is the concentration of oxygen in a subsurface layer. (In the STM model, $\alpha = 0$, and the vacant-site fraction is $1 - x - y - z$.) The kinetic parameters (preexponential constants and activation energies) are those suggested by Slinko et al. (1999) (except for k_{-1}, which was adjusted to $6.9 \cdot 10^9$ s^{-1} instead the original $6.0 \cdot 10^9$).

The heat balance accounts for accumulation, conduction, reaction, and heat transfer, assuming the fluid temperature (T_g) is fixed, while the gas-phase balance is described as a mixed reactor and accounts for flow (at a rate q measured at T_{ref}, $\tau_R = V/_q$) and reaction averaged over the catalyst, of surface area, S. These balances are of the form

$$\tau_T \frac{\partial T}{\partial t} - L_T^2 \nabla^2 T = (T_g - T) + B\Delta T_m R_{\mathrm{CO}}, \qquad T(R) = T_g$$

$$\tau_T = \frac{\rho_s C_{ps}}{h}; \qquad L_T^2 = \frac{\lambda_s}{h}; \qquad \Delta T_m = \frac{(-\Delta H) q P^0_{\mathrm{CO}}}{hSRT_{\mathrm{ref}}};$$

$$B = \frac{bSRT_{\mathrm{ref}}}{qP^0_{\mathrm{CO}}} \qquad (2)$$

$$\tau_R \frac{\partial P_{\mathrm{CO}}}{\partial t} = (P^0_{\mathrm{CO}} - P_{\mathrm{CO}}) - BP^0_{\mathrm{CO}}\langle R'_{\mathrm{CO}}\rangle \qquad (3)$$

where T and P_{CO} are the solid temperature (K) and reactant concentration (Pa), respectively. The heat-generation term should account for the three processes (oxygen and CO adsorption and surface reaction) and their corresponding enthalpy, but since they are equal for most of the cycle we choose, $R_{\mathrm{CO}} = k_r xy$ with the corresponding overall enthalpy as $(-\Delta H)$.

The transport parameters were estimated based on a surface density of 200 g/m^2 = 0.02 g/cm^2, leading to a heat capacity of 0.005 cal/(cm^2 K) and a solid thermal conductivity of 2.4×10^{-2} cal/(cm · s K). For cloth thickness of 0.02 cm, the characteristic front width is $L_T^2 = kd/h = 0.018$ cm^2 or $L_T = 0.14$ cm, and the dimensionless system size is about 15. The corresponding thermal time scale is $\tau_{\mathrm{T}} = 0.03$ min ~ 2 s. Front velocity will be 0.1 cm/s, in order of magnitude, in qualitative agreement with experiments, and the time required to conquer the surface (18 mm) is about 20 s. That leaves two parameters to be estimated: the concentration of catalytic sites (b, Eq. 2), which affects the rate factor (BP^0_{CO}), and the temperature rise (ΔT_m): both should be estimated from experimental results.

The model predicts the following observed features (Figure 4): (a) The sustained patterns exhibit a breathing motion in which a hot spot expands and contracts continuously; (b) the temporally complex pattern can be classified as mixed-mode oscillations with a large relaxation-type conversion peak superimposed with several smaller peaks; (c) the number of such smaller peaks varies with operating conditions (the reactor temperature) and can be characterized by a mechanism of period-adding.

Numerical simulations of the lumped system (Nekhamkina

et al., 2003) map the domains of the simple and complex oscillations, and characterize the transition as either period-doubling or period-adding. Simulations of the full distributed system reveal the features just described and the nature of bifurcation to complexity. The simulations do not describe the maximal temperature gradient and the period of the oscillations. The latter can be easily corrected by adjusting the slow time scale (k_3 and k_4). Before we attempt estimating a systematic parameter estimation, we will try to predict some of the kinetic parameters (activation energies) from basic principles.

Conclusion

IRT studies of oscillatory behavior during catalytic oxidation of CO over Pd supported on a glass-fiber catalytic cloth were conducted in a continuous reactor with feed flowing perpendicular to and through the disk-shaped catalyst. Typical thermograms of sustained patterns exhibit a hot spot that expands and contracts continuously (a breathing pattern), in a temporal pattern that matched the oscillations in exit CO_2 concentration. The oscillations were of the complex relaxation type, with fast (1-min) oscillations superimposed on the active phase of the long (10–60-min) cycle. The novelty of these results lies in the pattern, which is well defined and amenable to systematic mathematical modeling, in the short period of the fast oscillations, which probably emerges due to the low heat capacity, as well as in the catalyst geometry, a disk-shaped cloth. Recent experiments in our group demonstrated that, when a 5-mm sintered-glass support is employed for the same reaction, the sharp front disappears, as do the high-frequency oscillations. The oscillations then exhibit the slow (1-h) period only, in agreement with other studies in the literature. That is expected, since the heat capacity and heat conductivity of the supported-glass catalyst are one to two orders of magnitude higher than those of the cloth support. This explains the main novelty of our study.

The features of the spatiotemporal patterns that were identified in this study make the modeling of this behavior quite straightforward. We constructed a model that capitalizes on published kinetic (isothermal) models for this reaction on a cloth catalyst (Slinko et al., 1999), and when coupled with a solid-phase enthalpy and gas-phase mass balances, predicts the main observed features of the pattern.

The well-defined patterns and the relatively fast oscillations make this reaction a good candidate for studying patterns in cylindrical reactors with flow in the axial or radial direction. This is the subject of our current experimentation.

Acknowledgment

This work was supported by the Volkswagen-Stiftung Foundation. The catalyst was prepared by Dr. Shyndler of our group. One of the authors (M.S.) is a member of the Minerva Center of Nonlinear Dynamics and Complex Systems. The other two authors (R.D. and O.N.) are partially supported by the Center for Absorption in Science, Ministry of Immigrant Absorption State of Israel.

Literature Cited

Annamalai, J., C. Ballandis, M. Somani, S. A. Liauw, and D. Luss, "Effect of Reactant Composition and Nonuniformities on Temperature Fronts," *J. Chem. Phys.,* **107**, 1896 (1997).

Barelko, V., I. I. Kurochka, A. G. Merzhanov, and K. G. Shkadinski, "Investigation of Traveling Waves on Catalytic Wires," *Chem. Eng. Sci.,* **33**, 805 (1978).

Chen, C. C., E. E. Wolf, and H. C. Chang, "Low-Dimensional Spatio-Temporal Thermal Dynamics on Nonuniform Catalytic Surfaces," *J. Phys. Chem.,* **97**, 1055 (1993).

Coombes, S., and A. H. Osbaldestin, "Period-Adding Bifurcations and Chaos in a Periodically Stimulated Excitable Neural Relaxation Oscillator," *Phys. Rev. E,* **62**, 4057 (2000).

Cordonier, G. A., and L. D. Schmidt, "Thermal Waves in NH_3 Oxidation on a Pt Wire," *Chem. Eng. Sci.,* **44**, 1983 (1989).

Elnashaie, S. S. E. H., H. M. Harraz, and M. E. Abashar, "Homoclinical Chaos and the Period-Adding Route to Complex Non-Chaotic Attractors in Fluidized Bed Catalytic Reactors," *Chaos, Solitons, Fractals,* **12**, 1761 (2001).

Ertl, G., "Oscillatory Catalytic Reactions at Single Crystal Surfaces," *Adv. Catal.,* **37**, 213 (1990).

Graham, M. D., S. L. Lane, and D. Luss, "Temperature Pulse Dynamics on a Catalytic Ring," *J. Phys. Chem.,* **97**, 7564 (1993).

Kellow, J. C., and E. E. Wolf, "Propagation of Oscillations During Ethylene Oxidation on a Rh/SiO_2 Catalyst," *AIChE J.,* **37**, 1844 (1991).

Keren, I., and M. Sheintuch, "Modeling and Analysis of Spatiotemporal Patterns in the Catalytic Converter with Oscillatory Kinetics," *Chem. Eng. Sci.,* **55**, 1461 (2000).

Lane, S. L., and D. Luss, "Rotating Temperature Pulse During Hydrogen Oxidation on a Nickel Ring," *Phys. Rev. Lett.,* **70**, 830 (1993).

Liauw, M. A., J. Ning, and D. Luss, "Pattern Formation on a Nonuniformly Active Ring," *J. Chem. Phys.,* **104**, 5657 (1996).

Lobban, L., and D. Luss, "Spatial Temperature Oscillations during Hydrogen Oxidation on a Nickel Foil," *J. Phys. Chem.,* **93**, 6530 (1989).

Marwaha, B., J. Annamalai, and D. Luss, "Hot Zone Formation During Carbon Monoxide Oxidation in a Radial Flow Reactor," *Chem. Eng. Sci.,* **56**, 89 (2001).

Matatov-Meytal, Y., and M. Sheintuch, "Hydrotreating Processes for Catalytic Abatement of Water Pollutants," *Catal. Today,* **75**, 63 (2002).

Middya, U., D. Luss, and M. Sheintuch, "Spatiotemporal Motions Due to Global Interaction," *J. Chem. Phys.,* **100**, 3568 (1994).

Middya, U., M. Sheintuch, M. D. Graham, and D. Luss, "Patterns of Temperature Pulses on Electrically Heated Catalytic Ribbons," *Physica D,* **63**, 393 (1993).

Nekhamkina, O., R. Digilov, and M. Sheintuch, "Modeling of Temporally-Complex Breathing Patterns During Pd-Catalyzed CO Oxidation," *J. Chem. Phys.,* **119,** 2322 (2003).

Philippou, G., F. Shultz, and D. Luss, "Spatiotemporal Temperature Patterns on an Electrically Heated Catalytic Ribbon," *J. Phys. Chem.,* **95**, 3224 (1991).

Philippou, G., M. Somani, and D. Luss, "Traveling Temperature Fronts on Catalytic Ribbons," *Chem. Eng. Sci.,* **48**, 2325 (1993).

Sales, B. C., J. E. Turner, and M. B. Maple, "Oscillatory Oxidation of CO over Pt, Pd and Ir Catalysts: Theory," *Surf. Sci.,* **114**, 381 (1982).

Schuth, F., B. E. Henry, and L. D. Schmidt, "Oscillatory Reactions in Heterogeneous Catalysis," *Adv. Catal.,* **39**, 51 (1993).

Sheintuch, M., "Spatiotemporal Structures of Controlled Catalytic Wires," *Chem. Eng. Sci.,* **44**, 1081 (1989).

Sheintuch, M., *J. Chem. Phys.,* **100**, 15137 (1996).

Sheintuch, M., and N. I. Jaeger, "Spatiotemporal Catalytic Patterns—Preface," *Catal. Today,* **70**, 285 (2001).

Sheintuch, M., and D. Luss, "Identification of Bifurcations and Centers in Systems with Complex Dynamic Behavior," *J. Chem. Phys.,* **93**, 5727 (1989).

Sheintuch, M., and O. Nekhamkina, "Reaction-Diffusion Patterns on a Disk or a Square in a Model with Long Range Interaction," *J. Chem. Phys.,* **107**, 8165 (1997).

Sheintuch, M., and R. A. Schmitz, "Oscillations in Catalytic Reactions," *Catal. Rev. Sci. Eng.,* **15**, 107 (1977).

Sheintuch, M., and S. Shvartsman, "Spatiotemporal Patterns in Catalytic Reactors," *AIChE J.,* **42**, 1041 (1996).

Shindler, Y., Y. Matatov-Meytal, and M. Sheintuch, "Wet Hydrochlorination of p-Chlorophenol Using Pd Supported on an Activated Carbon Cloth," *Ind. Eng. Chem. Res.,* **40**, 3301 (2001).

Slinko, M. M., and N. J. Jaeger, "Oscillatory Heterogeneous Catalytic Systems," *Studies in Surface Science and Catalysis*, Vol. 86, Elsevier, Amsterdam (1994).

Slinko, M. M., E. S. Hurkina, M. J. Liauw, and N. I. Jaeger, "Mathematical

Modeling of Complex Oscillatory behavior during CO Oxidation over Pd Zeolite Catalysts," *J. Chem. Phys.*, **111,** 8105 (1999).
Yuranov, I., L. Kiwi-Minsker, M. Slinko, E. Kurkina, E. D. Tolstunova, and A. Renken, "Oscillatory Behavior During CO Oxidation Over Pd Supported on Glass Fibers: Experimental Study and Mathematical Modeling," *Chem. Eng. Sci.,* **55**, 2827 (2000).

Manuscript received Feb. 20, 2003, and revision received May 18, 2003.